1994AJ....107.1189T

THE ASTRONOMICAL JOURNAL VOLUME 107, NUMBER 3 MARCH 1994

LIE–POISSON INTEGRATORS FOR RIGID BODY DYNAMICS IN THE SOLAR SYSTEM

JIHAD TOUMA
Department of Mathematics, Massachusetts Institute of Technology, Cambridge, Massachusetts 02139
Electronic mail: jihad@birkhoff.mit.edu

JACK WISDOM
Department of Earth, Atmospheric, and Planetary Sciences, Massachusetts Institute of Technology, Cambridge, Massachusetts 02139
Electronic mail: wisdom@poincare.mit.edu

Received 1992 November 17; revised 1993 September 29

ABSTRACT

The n-body mapping method of Wisdom & Holman [AJ, 102, 1528 (1991)] is generalized to encompass rotational dynamics. The Lie–Poisson structure of rigid body dynamics is discussed. Integrators which preserve that structure are derived for the motion of a free rigid body and for the motion of rigid bodies interacting gravitationally with mass points.

1. INTRODUCTION

There is a growing appreciation of the importance of understanding the dynamics of the solar system on very long time scales and there is no way to study this dynamics other than long-term numerical integration. Such computational journeys in the solar system are taking place with greater frequency. They have been made possible by improvements in computer hardware as well as improvements in numerical integration algorithms. As a recent example, Wisdom & Holman (1991, hereafter referred to as WH91) presented a new symplectic mapping method for integration of the planetary n-body problem which is an order of magnitude faster than conventional integrators. Sussman & Wisdom (1992) used the new mapping method with the Supercomputer Toolkit (Abelson *et al.* 1992), a specialized parallel supercomputer, to integrate the evolution of the whole solar system for 100 mil yr. That calculation confirmed the result of Laskar (1989) that the evolution of the solar system is chaotic with an exponential divergence time scale of only 4–5 mil yr. In this paper we extend the algorithmic developments of WH91 to encompass rigid body motion in the context of solar system dynamics. We introduce a symplectic scheme for integrating the motion of a free rigid body, which conserves the magnitude of the angular momentum vector and its orientation in space. Then, we incorporate gravitational interactions to obtain a symplectic scheme which integrates the motion of rigid bodies interacting gravitationally with mass points, while preserving the total angular momentum vector.

2. THE IDEA: DIVIDE AND CONQUER

As described in WH91, symplectic mappings analogous to the n-body mapping method can be generated for any problem for which the Hamiltonian can be split into parts which are individually integrable and efficiently solvable. Consider a Hamiltonian of the form

$$H=H_1+H_2, \tag{2.0.1}$$

where H_1 and H_2 are individually efficiently solvable. The simplest mapping is obtained by multiplying the perturbation H_2 by a periodic sequence of Dirac delta functions

$$H_{\rm map}=H_1+2\pi\delta_{2\pi}(\Omega t)H_2, \tag{2.0.2}$$

where

$$\delta_{2\pi}(t)=\sum_{n=-\infty}^{\infty}\delta(t-n2\pi)=\frac{1}{2\pi}\sum_{n=-\infty}^{\infty}\cos(nt), \tag{2.0.3}$$

and Ω is the mapping frequency, which is related to the step size h of the mapping by $\Omega=2\pi/h$. The motivation is the averaging principle: provided step size resonances are avoided (see Wisdom & Holman 1992, and below) the extra-high-frequency terms introduced by the delta functions tend to average out and do not contribute substantially to the evolution of the system. The advantage is that the evolution of the whole system can be computed in terms of the efficiently solvable pieces: between the delta functions the motion is entirely governed by H_1 and crossing the delta functions the evolution is governed solely by H_2. The simple mapping method, as just presented, is only accurate to first order in the step size, but has the correct average Hamiltonian. The mapping can be made accurate to second order while preserving the average Hamiltonian by offsetting the delta functions by half a mapping step. Higher order can be achieved by a more intricate interleaving of the evolutions governed by the integrable parts of the Hamiltonian. Of course, similar mappings can also be generated from Hamiltonians which are separated into more than two solvable parts, but achieving high order is more complicated, though perfectly straightforward. In what follows we concentrate on the efficient solution of parts of the Hamiltonian under the presumption that the method of putting them together to form the map of the desired order is understood.

Deriving a map for the problem of celestial rigid bodies appears to be a straightforward application of the proce-

 0004-6256/94/107(3)/1189/14/$0.90 © 1994 Am. Astron. Soc. 1189

© American Astronomical Society • Provided by the NASA Astrophysics Data System

1994AJ....107.1189T

dure just described. We write the full Hamiltonian as a sum of integrable pieces

$$H=H_{\text{Euler}}+H_{\text{Kepler}}+H_{\text{interaction}}, \tag{2.0.4}$$

where H_{Euler} describes the free rigid body motion of each extended body, H_{Kepler} describes the interaction of each body with the massive central object (which may be an extended body itself), and $H_{\text{interaction}}$ includes all remaining gravitational interactions. Each of the components is separately integrable, as required. The problem with this direct application of the mapping procedure is that though the motion of the rigid body is integrable, to our knowledge, it is not efficiently solvable. The solution is complex and involves elliptic functions (see Whittaker 1929).

We can avoid the use of elliptic functions by further dividing the Hamiltonian for the free rigid body into two integrable pieces: a part which describes the integrable motion of an axisymmetric rigid body and an integrable perturbation which describes the triaxial deviation from axisymmetry. This division is motivated by the near axisymmetry of many bodies in the solar system; however, the algorithm is not limited to such situations. The solutions of these subproblems are simple and free of elliptic integrals.

This approach still has further problems. A fundamental problem in the description of the motion of the rigid body is that any choice of canonical angles, such as Euler angles, is singular. A complete covering of the phase space without singularities requires at least two independent coordinate systems (see, e.g., Wisdom *et al.* 1984). So, we take Euler's advice and look at the motion of the angular momentum vector in a frame moving with the body. This move has the advantage of dealing with nonsingular Cartesian components, and, for the free rigid body, of looking at the dynamics on the sphere defined by the conserved angular momentum. We first solve for the evolution of the Cartesian components of the angular momentum vector in the rigid body frame and then recover the configuration via a set of kinematic equations. Euler's equations have three dimensions; the phase space of the rigid body is six dimensional. Euler's approach to rigid body dynamics is a particular case of a more general formalism which can be used to reduce the dimensionality of problems with symmetry, the Lie–Poisson formalism. We make use of the Lie–Poisson formalism to derive singularity free algorithms for the problem at hand.

3. GRAVITATING RIGID BODIES

The Hamiltonian of a rigid body gravitationally interacting with a mass point is the sum of the kinetic and potential energy. The kinetic energy of a rigid body can be written as the sum of the translational kinetic energy of the center of mass and the kinetic energy of rotation about the center of mass. The potential energy is that of an arbitrary mass distribution in the Newtonian field of a mass point. The Hamiltonian is given by

$$H=\frac{\mathbf{p}_1^2}{2m_1}+\frac{\mathbf{p}_2^2}{2m_2}+\frac{1}{2}\mathbf{M}\cdot\mathsf{I}^{-1}\mathbf{M}-\int_B\frac{Gm_1}{|\mathbf{r}+\mathsf{C}\mathbf{Q}|}\,dm(\mathbf{Q}), \tag{3.0.1}$$

where m_1, $\mathbf{r}_1$, and $\mathbf{p}_1$ are the mass, position, and linear momentum of the mass point S, and m_2, $\mathbf{r}_2$, and $\mathbf{p}_2$ are the mass, position of the center of mass, and the linear momentum of the rigid body B. The vector $\mathbf{r}$ is the relative position vector: $\mathbf{r}=\mathbf{r}_2-\mathbf{r}_1$, and $dm(\mathbf{Q})$ is a differential mass element of the body at position $\mathbf{Q}$. The vector $\mathbf{M}$ is the angular momentum of B, and I is the inertia tensor. C is the orthogonal matrix that situates the body frame $\mathscr{B}$ with respect to the inertial frame $\mathscr{S}$. We denote by lowercase letters vectors in the inertial frame $\mathscr{S}$ and by uppercase letters their counterparts in the rigid body frame $\mathscr{B}$. The generalization to more point masses or extended rigid bodies is straightforward and will be presented in later sections.

The Hamiltonian only depends on the relative positions of the bodies; a transformation to relative coordinates and center of mass coordinates separates the interesting relative dynamics from the trivial dynamics of the center of mass. The Hamiltonian for the relative motion is

$$H=\frac{\mathbf{p}^2}{2}\left(\frac{1}{m_1}+\frac{1}{m_2}\right)+\frac{1}{2}\mathbf{M}\cdot\mathsf{I}^{-1}\mathbf{M}-\int_B\frac{Gm_1}{|\mathbf{r}+\mathsf{C}\mathbf{Q}|}\,dm(\mathbf{Q}), \tag{3.0.2}$$

where $\mathbf{p}$ is the linear momentum conjugate to $\mathbf{r}$.

To derive the mapping we must separate the Hamiltonian into integrable pieces. We want to take advantage of the fact that the unperturbed motion consists of the composition of an elliptical two-body motion and of free rigid body motion governed by Euler's equations. With this in mind, we expand the potential function in terms of Legendre polynomials. For the applications we have in mind, it is sufficient to consider the first three terms. Higher order terms can be included without a substantial increase in computational effort. This procedure gives us McCullagh's formula (Danby 1988; Plummer 1960) for the potential, which when incorporated with the kinetic energy yields the Hamiltonian

$$H_2=\underbrace{\frac{\mathbf{p}^2}{2}\left(\frac{1}{m_1}+\frac{1}{m_2}\right)+\frac{1}{2}\mathbf{M}\cdot\mathsf{I}^{-1}\mathbf{M}-\frac{Gm_1m_2}{r}}_{H_{\text{free}}}$$
$$\underbrace{-\frac{Gm_1}{2r^3}\operatorname{tr}(\mathsf{I})+\frac{3}{2}\frac{Gm_1}{r^5}\mathbf{R}\cdot\mathsf{I}\mathbf{R}}_{H_{\text{interaction}}}. \tag{3.0.3}$$

In H_{free}, the rotational and translational motions decouple. We write

$$H_{\text{free}}=H_{\text{Kepler}}+H_{\text{Euler}}, \tag{3.0.4}$$

where

© American Astronomical Society • Provided by the NASA Astrophysics Data System

1994AJ....107.1189T

$$H_{\text{Kepler}}=\frac{\mathbf{p}^2}{2}\left(\frac{1}{m_1}+\frac{1}{m_2}\right)-\frac{Gm_1m_2}{r},$$

$$H_{\text{Euler}}=\tfrac{1}{2}\mathbf{M}\cdot\mathsf{I}^{-1}\mathbf{M}. \tag{3.0.5}$$

We diagonalize I by choosing the principal axis frame as the body frame, and denote by I_1, I_2, and I_3 the moments of inertia about the principal axes oX, oY, and oZ, respectively. In the principal axis frame the rigid body Hamiltonian is

$$H_{\text{Euler}}=\frac{M_1^2}{2I_1}+\frac{M_2^2}{2I_2}+\frac{M_3^2}{2I_3}, \tag{3.0.6}$$

where M_1, M_2, and M_3 denote the components of the angular momentum on the principal axes.

As outlined earlier, we divide the rigid body Hamiltonian into two sub-Hamiltonians

$$H_{\text{Euler}}=\underbrace{\frac{M_1^2+M_2^2}{2I_2}+\frac{M_3^2}{2}}_{H_{\text{axisymmetric}}}+\underbrace{\frac{M_1^2}{2}\left(\frac{1}{I_1}-\frac{1}{I_2}\right)}_{H_{\text{triaxial}}}. \tag{3.0.7}$$

$H_{\text{axisymmetric}}$ governs the motion of an axisymmetric body, and H_{triaxial} acts as a perturbation. This splitting is motivated by applications in solar system dynamics where departures from axisymmetry are often small, though the application of the mapping is not limited to problems with small triaxiality.

We must find efficiently computable solutions to each piece of the Hamiltonian. We first present a canonical version of the rigid body mapping, and then turn to the Lie–Poisson formalism.

4. CANONICAL MAP FOR THE FREE RIGID BODY

In this section the pieces of the free rigid body Hamiltonian are integrated in a convenient set of canonical coordinates, the Andoyer coordinates (Andoyer 1923; Deprit 1967). The Andoyer momenta have simple physical interpretations in terms of the angular momentum and its projections in the body and inertial reference frames. In Andoyer variables the free rigid body Hamiltonian is cyclic in the coordinate conjugate to the total angular momentum; thus Andoyer variables naturally express the conservation of total angular momentum. This property is not shared by the traditional Euler angles. A further advantage of the Andoyer variables is that $H_{\text{axisymmetric}}$ and H_{triaxial} are easily solved when expressed in terms of them.

We denote by $oxyz$ an inertial reference frame and by $oXYZ$ a frame rotating with the rigid body. Let $\mathbf{M}$ be the angular momentum vector as seen in the body frame, and Γ the plane normal to the angular momentum vector $\mathbf{M}$. The canonical system consists of the momenta

- F, the projection of $\mathbf{M}$ on oz;
- G, the magnitude of $\mathbf{M}$;
- L, the projection of $\mathbf{M}$ on oZ,

and the angles conjugate to them:

- f, the angle between ox and the line of intersection of Γ with oxy.
- g, the angle between the lines of intersection of Γ with oxy and oXY;
- l, the angle between the line of intersection of Γ with oXY and oX.

From the definitions, it follows that

$$\begin{aligned} M_1&=\sqrt{G^2-L^2}\sin(l),\\ M_2&=\sqrt{G^2-L^2}\cos(l),\\ M_3&=L, \end{aligned} \tag{4.0.1}$$

where M_1, M_2, and M_3 are the components of $\mathbf{M}$ along oX, oY, and oZ, respectively. Using these we can reexpress the rigid body Hamiltonian in terms of the Andoyer variables

$$H_{\text{Euler}}=\underbrace{\frac{G^2}{2I_2}+\frac{L^2}{2}\left(\frac{1}{I_3}-\frac{1}{I_2}\right)}_{H_{\text{axisymmetric}}}+\underbrace{\frac{(G^2-L^2)\sin^2(l)}{2}\left(\frac{1}{I_1}-\frac{1}{I_2}\right)}_{H_{\text{triaxial}}}. \tag{4.0.2}$$

The equations of motion are derived via Hamilton's equations or equivalently the canonical Poisson bracket. We solve $H_{\text{axisymmetric}}$ and H_{triaxial} separately, and then approximate the solutions of H_{Euler} with the method outlined above.

The Hamiltonian $H_{\text{axisymmetric}}$ is cyclic in all the coordinates, so the momenta are conserved

$$\begin{aligned} L(t)&=L(0),\\ l(t)&=L(0)\left(\frac{1}{I_3}-\frac{1}{I_2}\right)t+l(0), \end{aligned} \tag{4.0.3}$$

and

$$\begin{aligned} G(t)&=G(0),\\ g(t)&=\frac{G(0)}{I_2}t+g(0). \end{aligned} \tag{4.0.4}$$

Of course, F, which is a spatial component, is conserved, and with it the angle f.

The Hamiltonian H_{triaxial} is independent of F, and cyclic in g and f, so $G(t)=G(0)$, $F(t)=F(0)$, and $f(t)=f(0)$. The other variables must satisfy

$$\begin{aligned} \frac{d}{dt}l&=\frac{\partial}{\partial L}H_{\text{triaxial}}=-\beta L\sin^2(l),\\ \frac{d}{dt}L&=-\frac{\partial}{\partial l}H_{\text{triaxial}}=-\beta(G^2-L^2)\sin(l)\cos(l),\\ \frac{d}{dt}g&=\frac{\partial}{\partial G}H_{\text{triaxial}}=\beta G\sin^2(l), \end{aligned} \tag{4.0.5}$$

where $\beta=1/I_1-1/I_2$.

We can integrate these equations as follows:

© American Astronomical Society • Provided by the NASA Astrophysics Data System

1994AJ....107.1189T

$$l(t)=\arctan\left(\frac{M_1(0)}{M_2(0)\cos(\nu t)+M_3(0)\sin(\nu t)}\right),$$
$$L(t)=-M_2(0)\sin(\nu t)+M_3(0)\cos(\nu t), \tag{4.0.6}$$
$$g(t)=\arctan\left(\frac{M_3^2(0)\sin(\nu t)+M_1^2(0)\sin(\nu t)+M_2(0)M_3(0)\cos(\nu t)}{M_1(0)M(0)\cos(\nu t)}\right),$$

where $M_1(0)$, $M_2(0)$, $M_3(0)$, and $M(0)$ are the initial values of the the angular momentum components and magnitude which we can compute in terms of $l(0)$, $L(0)$, and $G(0)$, and $\nu=\beta M_1(0)$. These are the equations of a rotation about the X axis expressed in canonical coordinates.

Having solved for the flows generated by $H_{\text{axisymmetric}}$ and H_{triaxial} we can use our method to construct approximations of the trajectories generated by H_{Euler} to the desired accuracy. Note that the transformations are symplectic (canonical) and they explicitly conserve G and F.

5. DO THE RIGHT THING: EULER'S MOVE

A while ago, Euler demonstrated the simplicity of rigid body dynamics when seen in a frame that is rotating with the body. In the absence of external forces, the angular momentum vector is fixed in space, and the motion of the body can be recovered by following the projections of that vector on a basis fixed in the body (Arnold 1978).

The configuration of the rigid body is specified by a special orthogonal transformation, $\mathsf{C}\in SO(3)$ which takes body vectors into space vectors

$$\mathbf{v}=\mathsf{C}\mathbf{V}. \tag{5.0.1}$$

Since no torques are acting on the body, the angular momentum vector $\mathbf{m}$ is invariant in space

$$\frac{d}{dt}\mathbf{m}=0, \tag{5.0.2}$$

or,

$$\frac{d}{dt}(\mathsf{C}\mathbf{M})=\mathsf{C}\frac{d}{dt}\mathbf{M}+\left(\frac{d}{dt}\mathsf{C}\right)\mathbf{M}=0. \tag{5.0.3}$$

For any time-dependent orthogonal matrix $\mathsf{C}(t)$, $[(d/dt)\mathsf{C}]\mathsf{C}^{-1}$ is skew symmetric, and, in the case of a rigid body, corresponds to the space angular velocity vector, $\boldsymbol{\omega}$:

$$\left(\frac{d}{dt}\mathsf{C}\right)\mathsf{C}^{-1}\mathbf{v}=\boldsymbol{\omega}\times\mathbf{v}. \tag{5.0.4}$$

The body angular velocity vector is given by $\boldsymbol{\Omega}=\mathsf{C}^{-1}\boldsymbol{\omega}$. Equation (5.0.3) reduces to

$$\frac{d}{dt}\mathbf{M}=\mathbf{M}\times\boldsymbol{\Omega}. \tag{5.0.5}$$

The angular momentum and velocity vectors are related by the symmetric moment of inertia tensor I:

$$\mathbf{M}=\mathsf{I}\boldsymbol{\Omega}. \tag{5.0.6}$$

So, we can rewrite Eq. (5.0.5) as

$$\frac{d}{dt}\mathbf{M}=\mathbf{M}\times\mathsf{I}^{-1}\mathbf{M}. \tag{5.0.7}$$

Euler's equations, as these equations are known, put us directly on the angular momentum sphere and are free of singularities.

To get the time evolution of $\mathscr{B}$ with respect to $\mathscr{S}$, we need to follow $\mathsf{C}(t)$. We can do it directly by solving for the configuration matrix

$$\frac{d}{dt}\mathsf{C}=\mathsf{C}\mathsf{S}[\mathsf{I}^{-1}\mathbf{M}], \tag{5.0.8}$$

where we denote by $\mathsf{S}[\mathbf{V}]$ the skew symmetric matrix associated with $\mathbf{V}$:

$$\mathsf{S}[\mathbf{V}]=\begin{pmatrix}0 & -V_3 & V_2\\ V_3 & 0 & -V_1\\ -V_2 & V_1 & 0\end{pmatrix}. \tag{5.0.9}$$

Alternatively, one can take an indirect route and follow the motion of a spatially fixed vector in the body frame. We adopt the second course since it fits naturally in the problem we are considering. Let $\mathbf{r}$ be an arbitrary vector fixed in $\mathscr{S}$:$\mathbf{R}=\mathsf{C}^{-1}\mathbf{r}$. Since $d/(dt)\mathbf{r}=0$, the motion of $\mathbf{R}$ is governed by

$$\frac{d}{dt}\mathbf{R}=\mathbf{R}\times\boldsymbol{\Omega}=\mathbf{R}\times\mathsf{I}^{-1}\mathbf{M}. \tag{5.0.10}$$

Clearly at any time t, we have $\mathbf{R}(t)=\mathsf{C}^{-1}(t)\mathbf{r}=\mathsf{C}^{-1}(t)\mathsf{C}(0)\mathbf{R}(0)$. So, by solving Eq. (5.0.10), we isolate $\mathsf{C}^{-1}(t)$, and recover the configuration matrix $\mathsf{C}(t)$ by transposition.

In summary, the motion of a rigid body is governed by the equations

$$\frac{d}{dt}\mathbf{M}=\mathbf{M}\times\mathsf{I}^{-1}\mathbf{M},$$
$$\frac{d}{dt}\mathbf{R}=\mathbf{R}\times\mathsf{I}^{-1}\mathbf{M}. \tag{5.0.11}$$

6. LIE–POISSON DYNAMICS

An interesting feature of Euler's equations is that the rate of change of the components of the angular momentum is expressible solely in terms of the components of the angular momentum. Even though the phase space of the

© American Astronomical Society • Provided by the NASA Astrophysics Data System

1994AJ....107.1189T

rigid body is six dimensional, the dynamics governing the angular momentum is only three dimensional. Now, the rate of change of any component of the angular momentum can be written as a Poisson bracket of that component with the rigid body Hamiltonian. Euler's equations show that the resulting Poisson bracket can be written solely in terms of the angular momentum. It turns out that a more general property holds: The Poisson bracket of any two functions of the angular momentum can be written solely in terms of the angular momentum. This property was known to Sophus Lie, and was first discussed in modern terms by Arnold (1966). Here, we give a coordinate-dependent proof of this interesting feature which we shall use later to connect functions defined on the angular momentum sphere to the dynamics they generate.

The Cartesian components of **M** were expressed as functions of the canonical Andoyer variables in Eqs. (4.0.1). The Poisson bracket of the components of the angular momentum with an arbitrary function of the angular momentum $F(\mathbf{M})$ is

$$\begin{aligned}\{M_1,F(\mathbf{M})\}&=\frac{\partial}{\partial l}M_1\frac{\partial}{\partial L}F(\mathbf{M})-\frac{\partial}{\partial L}M_1\frac{\partial}{\partial l}F(\mathbf{M}),\\ \{M_2,F(\mathbf{M})\}&=\frac{\partial}{\partial l}M_2\frac{\partial}{\partial L}F(\mathbf{M})-\frac{\partial}{\partial L}M_2\frac{\partial}{\partial l}F(\mathbf{M}),\\ \{M_3,F(\mathbf{M})\}&=\frac{\partial}{\partial l}M_3\frac{\partial}{\partial L}F(\mathbf{M})-\frac{\partial}{\partial L}M_3\frac{\partial}{\partial l}F(\mathbf{M}).\end{aligned}\tag{6.0.1}$$

We carry out the computations explicitly for M_1 and derive the others by analogy. We have

$$\begin{aligned}\frac{\partial}{\partial l}F&=\nabla_{\mathbf{M}}F\frac{\partial}{\partial l}\mathbf{M},\\ \frac{\partial}{\partial L}F&=\nabla_{\mathbf{M}}F\frac{\partial}{\partial L}\mathbf{M},\end{aligned}\tag{6.0.2}$$

where $\nabla_{\mathbf{M}}$ refers to the gradient with respect to the components of **M**. Using Eqs. (4.0.1), we obtain

$$\begin{aligned}\frac{\partial}{\partial l}\mathbf{M}&=\begin{pmatrix}M_2\\-M_1\\0\end{pmatrix}\\ \frac{\partial}{\partial L}\mathbf{M}&=\begin{pmatrix}-\dfrac{M_3M_1}{M_1^2+M_2^2}\\-\dfrac{M_3M_2}{M_1^2+M_2^2}\\1\end{pmatrix}.\end{aligned}\tag{6.0.3}$$

Replacing in the equation for M_1, we obtain

$$\begin{aligned}&\{M_1,F(\mathbf{M})\}\\ &=M_2\left(-\frac{\partial F}{\partial M_1}\frac{M_3M_1}{M_1^2+M_2^2}-\frac{\partial F}{\partial M_2}\frac{M_3M_2}{M_1^2+M_2^2}+\frac{\partial F}{\partial M_3}\right)\\ &\quad+\frac{M_3M_1}{M_1^2+M_2^2}\left(M_2\frac{\partial}{\partial M_1}F-M_1\frac{\partial}{\partial M_2}F\right),\end{aligned}\tag{6.0.4}$$

which after reduction gives

$$\{M_1,F(\mathbf{M})\}=M_2\frac{\partial F}{\partial M_3}-M_3\frac{\partial F}{\partial M_2}.\tag{6.0.5}$$

Similarly, we find that

$$\begin{aligned}\{M_2,F(\mathbf{M})\}&=M_3\frac{\partial F}{\partial M_1}-M_1\frac{\partial F}{\partial M_3},\\ \{M_3,F(\mathbf{M})\}&=M_1\frac{\partial F}{\partial M_2}-M_2\frac{\partial F}{\partial M_1}.\end{aligned}\tag{6.0.6}$$

Thus, we are able to express the canonical Poisson bracket of **M** with any real valued function F of **M**, in terms of **M** alone:

$$\{\mathbf{M},F\}=\mathbf{M}\times\nabla_{\mathbf{M}}F.\tag{6.0.7}$$

In particular, when F is equal to H_{Euler}, $\nabla_{\mathbf{M}}F=\mathsf{I}^{-1}\mathbf{M}$ and

$$\frac{d}{dt}\mathbf{M}=\{\mathbf{M},F(\mathbf{M})\}=\mathbf{M}\times\mathsf{I}^{-1}\mathbf{M},\tag{6.0.8}$$

which is Euler's equation.

We can generalize this computation by finding the Poisson bracket of two arbitrary real valued functions F_1 and F_2 of **M**. The time derivative of F_1 along the trajectories generated by F_2 is given by

$$\begin{aligned}\frac{d}{dt}F_1&=\nabla_{\mathbf{M}}F_1\cdot\frac{d}{dt}\mathbf{M}=\nabla_{\mathbf{M}}F_1\cdot(\mathbf{M}\times\nabla_{\mathbf{M}}F_2)\\ &=-\mathbf{M}\cdot(\nabla_{\mathbf{M}}F_1\times\nabla_{\mathbf{M}}F_2).\end{aligned}\tag{6.0.9}$$

Thus,

$$\{F_1,F_2\}=-\mathbf{M}\cdot(\nabla_{\mathbf{M}}F_1\times\nabla_{\mathbf{M}}F_2).\tag{6.0.10}$$

We can recover the equation governing the motion of a spatially fixed vector in the body frame within this formalism. We start by generalizing the configuration Eq. (5.0.8) to the case of the flow generated by an arbitrary Hamiltonian $F(\mathbf{M})$. Using Eq. (6.0.7), we rewrite Eq. (5.0.3) as

$$\mathsf{C}(\mathbf{M}\times\nabla_{\mathbf{M}}F)+\left(\frac{d}{dt}\mathsf{C}\right)\mathbf{M}=0.\tag{6.0.11}$$

Using the fact that this equation holds for any **M**, we find

$$\frac{d}{dt}\mathsf{C}=\mathsf{C}\mathsf{S}[\nabla_{\mathbf{M}}F].\tag{6.0.12}$$

Next, we consider an arbitrary space fixed vector $\mathbf{r}=\mathsf{C}\mathbf{R}$. As before, we can write

$$\mathsf{C}\frac{d}{dt}\mathbf{R}+\left(\frac{d}{dt}\mathsf{C}\right)\mathbf{R}=0.\tag{6.0.13}$$

Using Eq. (6.0.12), we obtain

$$\frac{d}{dt}\mathbf{R}=-\mathsf{S}[\nabla_{\mathbf{M}}F]\mathbf{R}.\tag{6.0.14}$$

Expanding the matrix multiplication, we get

$$\frac{d}{dt}\mathbf{R}=\{\mathbf{R},F(\mathbf{M})\}=\mathbf{R}\times\nabla_{\mathbf{M}}F.\tag{6.0.15}$$

© American Astronomical Society • Provided by the NASA Astrophysics Data System

1994AJ....107.1189T

As before, when $F(\mathbf{M})$ is equal to H_{Euler}, we get the expected equation for $\mathbf{R}$:

$$\frac{d}{dt}\mathbf{R}=\mathbf{R}\times\nabla_{\mathbf{M}}H_{\text{Euler}}=\mathbf{R}\times\mathbf{I}^{-1}\mathbf{M}. \tag{6.0.16}$$

Note that for any Hamiltonian H, which only depends on $\mathbf{M}$, the equations of motion generated by the Poisson bracket conserves the magnitude of $\mathbf{R}$:

$$\mathbf{R}\cdot\frac{d}{dt}\mathbf{R}=\mathbf{R}\cdot(\mathbf{R}\times\nabla_{\mathbf{M}}H)=0. \tag{6.0.17}$$

The same is true for $\mathbf{M}$. So, for any such H, the motion of $\mathbf{M}$ and $\mathbf{R}$ consists of finite rotations.

The reduction procedure is not specific to the free rigid body problem. A reduction of the Poisson bracket from a high-dimensional phase space to one of lower dimensions, is possible whenever a group of symmetries acts on the original phase space. In the case that the phase space is the cotangent bundle of a Lie group, and the symmetry group is the Lie group itself, the reduction procedure leads to what is known as the Lie–Poisson bracket. This is precisely the case of the free rigid body problem where the configuration space is the group of special orthogonal transformations and the dual Lie algebra can be identified with the angular momentum space. In Sec. *6.1*, we derive a Lie–Poisson bracket for the problem of a rigid body interacting gravitationally with a mass point, a problem which is invariant under the group of Euclidean motions.

6.1 Spin-Orbit Lie–Poisson Bracket

Hamiltonian Eq. (3.0.2), the spin-orbit Hamiltonian, admits the group of Euclidean motions as a group of symmetry. This translates into the conservation of the total linear and angular momenta. We used the conservation of linear momentum when we moved to the center of mass frame. In order to enforce the rotational symmetry, we move to $\mathscr{B}$. Denoting vectors in the body by capital letters as before, $\mathbf{R}$ is the relative vector in the rigid body frame, and $\mathbf{P}$ is the relative linear momentum in the body frame. The equations of motion, including the kinematic accelerations, are

$$\begin{aligned}
\frac{d}{dt}\mathbf{P}&=\mathbf{P}\times\mathbf{I}^{-1}\mathbf{M}-\int_B\frac{Gm_1(\mathbf{R}+\mathbf{Q})}{|\mathbf{R}+\mathbf{Q}|^3}\,dm(\mathbf{Q}),\\
\frac{d}{dt}\mathbf{R}&=\mathbf{R}\times\mathbf{I}^{-1}\mathbf{M}+\mathbf{P}\left(\frac{1}{m_1}+\frac{1}{m_2}\right),\\
\frac{d}{dt}\mathbf{M}&=\mathbf{M}\times\mathbf{I}^{-1}\mathbf{M}+\int_B\frac{Gm_1(\mathbf{R}\times\mathbf{Q})}{|\mathbf{R}+\mathbf{Q}|^3}\,dm(\mathbf{Q}).
\end{aligned} \tag{6.1.1}$$

After our discussion of Euler's equations, the reader should not be surprised to find out that these equations can be derived via a Poisson bracket of the various dynamic variables with the Hamiltonian expressed in the body frame

$$\hat{H}=\frac{\mathbf{P}^2}{2}\left(\frac{1}{m_1}+\frac{1}{m_2}\right)+\frac{1}{2}\mathbf{M}\cdot\mathbf{I}^{-1}\mathbf{M}-\int_B\frac{Gm_1}{|\mathbf{R}+\mathbf{Q}|}\,dm(\mathbf{Q}). \tag{6.1.2}$$

A formal derivation of the bracket, which uses the differential structure of the Lie group of Euclidean motions, is given in Wang *et al.* (1991). Here, we derive the bracket in a manner analogous to our derivation of the Lie–Poisson bracket for the free rigid body. To give an idea of what is involved, we derive the equations of the angular momentum vector. As argued before, we can express the angular momentum vector in terms of canonical variables. The canonical equations governing the evolution of $\mathbf{M}$ are

$$\frac{d}{dt}\mathbf{M}=\{\mathbf{M},H\}, \tag{6.1.3}$$

where the bracket denotes the canonical Poisson bracket. Applying the chain rule, we expand the Poisson bracket:

$$\begin{aligned}
\{\mathbf{M},H\}=\{\mathbf{M},\hat{H}\}=\mathbf{M}\times\nabla_{\mathbf{M}}\hat{H}&-\sum_{i=1}^{3}[\nabla_{\mathbf{R}}\hat{H}\cdot\{\mathbf{R},M_i\}]\mathbf{e}_i\\
&-\sum_{i=1}^{3}[\nabla_{\mathbf{P}}\hat{H}\cdot\{\mathbf{P},M_i\}]\mathbf{e}_i,
\end{aligned} \tag{6.1.4}$$

where $\mathbf{e}_1$, $\mathbf{e}_2$, and $\mathbf{e}_3$ are unit vectors along axes oX, oY, and oZ, respectively. The $\mathbf{M}$ dependence of $\hat{H}$ gives the term $\mathbf{M}\times\nabla_{\mathbf{M}}\hat{H}$ as shown before. Using Eq. (6.0.15), we get

$$\begin{aligned}
\{\mathbf{R},M_i\}&=\mathbf{R}\times\nabla_{\mathbf{M}}M_i=\mathbf{R}\times\mathbf{e}_i,\\
\{\mathbf{P},M_i\}&=\mathbf{P}\times\nabla_{\mathbf{M}}M_i=\mathbf{P}\times\mathbf{e}_i,\quad i=1,2,3.
\end{aligned} \tag{6.1.5}$$

Replacing in Eq. (6.1.4) we get

$$\frac{d}{dt}\mathbf{M}=\{\mathbf{M},\hat{H}\}=\mathbf{M}\times\nabla_{\mathbf{M}}\hat{H}+\mathbf{R}\times\nabla_{\mathbf{R}}\hat{H}+\mathbf{P}\times\nabla_{\mathbf{P}}\hat{H}. \tag{6.1.6}$$

The canonical structure, in addition to the reduction calculations, gives us the remaining equations for $\mathbf{R}$ and $\mathbf{P}$ in terms of a Poisson bracket

$$\begin{aligned}
\frac{d}{dt}\mathbf{R}&=\mathbf{R}\times\nabla_{\mathbf{M}}\hat{H}+\nabla_{\mathbf{P}}\hat{H},\\
\frac{d}{dt}\mathbf{P}&=\mathbf{P}\times\nabla_{\mathbf{M}}\hat{H}-\nabla_{\mathbf{R}}\hat{H}.
\end{aligned} \tag{6.1.7}$$

If $\hat{H}$ happens to be the spin-orbit coupling Hamiltonian, expressed in the rigid body frame, we get the expected equations for the motion of $\mathbf{M}$, $\mathbf{R}$, and $\mathbf{P}$.

Note that for any $\hat{H}(\mathbf{R},\mathbf{P},\mathbf{M})$, these equations preserve the total angular momentum

$$\mathbf{m}_{\text{total}}=\mathbf{m}+\mathbf{r}\times\mathbf{p}, \tag{6.1.8}$$

as can be seen by taking the time derivative of $\mathbf{m}_{\text{total}}$ and replacing $(d/dt)\mathbf{M}$, $(d/dt)\mathbf{R}$, and $(d/dt)\mathbf{P}$ with the Poisson brackets just derived.

Finally, we derive the Poisson bracket of two real valued functions, F_1 and F_2, of $\mathbf{M}$, $\mathbf{R}$, and $\mathbf{P}$:

© American Astronomical Society • Provided by the NASA Astrophysics Data System

1994AJ....107.1189T

$$\{F_1,F_2\}=\nabla_{\mathbf{M}}F_1\cdot\{\mathbf{M},F_2\}+\nabla_{\mathbf{R}}F_1\cdot\{\mathbf{R},F_2\}+\nabla_{\mathbf{P}}F_1\cdot\{\mathbf{P},F_2\}$$
$$=-\mathbf{M}\cdot[\nabla_{\mathbf{M}}F_1\times\nabla_{\mathbf{M}}F_2]+\mathbf{R}\cdot[\nabla_{\mathbf{R}}F_2\times\nabla_{\mathbf{M}}F_1$$
$$-\nabla_{\mathbf{R}}F_1\times\nabla_{\mathbf{M}}F_2]+\mathbf{P}\cdot[\nabla_{\mathbf{P}}F_2\times\nabla_{\mathbf{M}}F_1$$
$$-\nabla_{\mathbf{P}}F_1\times\nabla_{\mathbf{M}}F_2]+\nabla_{\mathbf{R}}F_1\cdot\nabla_{\mathbf{P}}F_2-\nabla_{\mathbf{P}}F_1\cdot\nabla_{\mathbf{R}}F_2. \quad (6.1.9)$$

With this, we end our adventure on Poisson manifolds. We will use the bracket derived in this section in the rest of the paper.

7. A LIE–POISSON MAPPING FOR A FREE RIGID BODY

We use the Lie–Poisson bracket to derive a scheme that integrates the motion of a free rigid body, while preserving the symplectic structure (Poisson bracket) and the magnitude of the angular momentum vector. The angular momentum vector is naturally fixed in space. First, we integrate the Hamiltonians that enter into the construction. Then, we put the integral curves together to approximate the actual motion.

7.1 Axisymmetric Body: Exact Solution

We solve for the motion of an axisymmetric body. Assume, for definiteness, that the body is symmetric about the Z axis, i.e., $I_1=I_2=I$. The Hamiltonian is given by

$$H=\frac{M_1^2+M_2^2}{2I}+\frac{M_3^2}{2I_3}. \quad (7.1.1)$$

Euler's equations become

$$\frac{d}{dt}M_1=M_3M_2\left(\frac{1}{I_3}-\frac{1}{I}\right),$$
$$\frac{d}{dt}M_2=-M_1M_3\left(\frac{1}{I_3}-\frac{1}{I}\right), \quad (7.1.2)$$
$$\frac{d}{dt}M_3=0.$$

These equations govern the precession of the angular momentum vector around the axis of symmetry. Setting $\alpha=(1/I_3-1/I)M_3(0)$, we integrate to get

$$\mathbf{M}(t)=\begin{pmatrix}\cos(\alpha t) & \sin(\alpha t) & 0\\ -\sin(\alpha t) & \cos(\alpha t) & 0\\ 0 & 0 & 1\end{pmatrix}\mathbf{M}(0)=\mathsf{C}_Z(\alpha t)\mathbf{M}(0). \quad (7.1.3)$$

Next, we solve for the motion of $\mathbf{R}$:

$$\frac{d}{dt}\mathbf{R}=\mathbf{R}\times\mathsf{I}^{-1}\mathbf{M}(t), \quad (7.1.4)$$

or, using Eq. (7.1.3)

$$\frac{d}{dt}\mathbf{R}=\mathbf{R}\times\mathsf{I}^{-1}\mathsf{C}_Z(\alpha t)\mathbf{M}(0). \quad (7.1.5)$$

It is easy to check that, in the case we are considering, $\mathsf{I}^{-1}\mathsf{C}_Z=\mathsf{C}_Z\mathsf{I}^{-1}$. Next, transform to a frame that is precessing with $\mathbf{M}$:

$$\mathbf{R}(t)=\mathsf{C}_Z(\alpha t)\mathbf{R}_p(t). \quad (7.1.6)$$

Replacing in Eq. (7.1.5), we get

$$\left(\frac{d}{dt}\mathsf{C}_Z\right)\mathbf{R}_p+\mathsf{C}_Z\frac{d}{dt}\mathbf{R}_p=\mathsf{C}_Z\mathbf{R}_p\times[\mathsf{C}_Z\mathsf{I}^{-1}\mathbf{M}(0)]. \quad (7.1.7)$$

Noting that $\mathsf{C}_Z a\times\mathsf{C}_Z b=\mathsf{C}_Z(a\times b)$, and that $\mathsf{C}_Z^{-1}=\mathsf{C}_Z^T$, we can rewrite Eq. (7.1.7) as follows:

$$\frac{d}{dt}\mathbf{R}_p=\mathbf{R}_p\times\mathsf{I}^{-1}\mathbf{M}(0)-\mathsf{C}_Z^T\left(\frac{d}{dt}\mathsf{C}_Z\right)\mathbf{R}_p. \quad (7.1.8)$$

But,

$$\mathsf{C}_Z^T\frac{d}{dt}\mathsf{C}_Z=\begin{pmatrix}0 & \alpha & 0\\ -\alpha & 0 & 0\\ 0 & 0 & 0\end{pmatrix}. \quad (7.1.9)$$

So, reducing the right-hand side of Eq. (7.1.8), we end up with

$$\frac{d}{dt}\mathbf{R}_p=\begin{pmatrix}0 & \frac{M_3(0)}{I} & -\frac{M_2(0)}{I}\\ -\frac{M_3(0)}{I} & 0 & \frac{M_1(0)}{I}\\ \frac{M_2(0)}{I} & -\frac{M_1(0)}{I} & 0\end{pmatrix}\mathbf{R}_p$$
$$=\mathbf{R}_p\times\frac{\mathbf{M}(0)}{I}. \quad (7.1.10)$$

These equations govern the precession of the vector $\mathbf{R}_p$ around the vector $\boldsymbol{\Omega}(0)=\mathbf{M}(0)/I$. The solution is given by the Euler–Rodrigues formula (see Goldstein 1980)

$$\mathbf{R}_p(t)=\mathsf{C}_{\boldsymbol{\Omega}}(\beta t)\mathbf{R}_p(0), \quad (7.1.11)$$

where

$$\mathsf{C}_{\boldsymbol{\Omega}}(\beta t)=\cos(\beta t)\mathsf{1}+\frac{\sin(\beta t)}{\beta}\mathsf{S}[\boldsymbol{\Omega}(0)]$$
$$+\frac{1-\cos(\beta t)}{\beta^2}\mathsf{S}^2[\boldsymbol{\Omega}(0)], \quad (7.1.12)$$

where $\mathsf{1}$ is the identity matrix, $\beta=-|\boldsymbol{\Omega}(0)|$, and $\mathsf{S}[\boldsymbol{\Omega}(0)]$ is the skew symmetric matrix corresponding to $\boldsymbol{\Omega}(0)$. Thus, we obtain

$$\mathbf{R}(t)=[\mathsf{C}_Z(\alpha t)\mathsf{C}_{\boldsymbol{\Omega}}(\beta t)]\mathbf{R}(0). \quad (7.1.13)$$

Finally, we update the configuration of the rigid body via

$$\mathsf{C}(t)=\mathsf{C}(0)[\mathsf{C}_{\boldsymbol{\Omega}}^{-1}(\beta t)\mathsf{C}_Z^{-1}(\alpha t)]. \quad (7.1.14)$$

7.2 Integrating Quadratic Monomials

The sub-Hamiltonian H_{triaxial} is of the form

$$H_{M_i}=\alpha_i\frac{M_i^2}{2},\quad i=1,2,3. \quad (7.2.1)$$

© American Astronomical Society • Provided by the NASA Astrophysics Data System

1994AJ....107.1189T

We solve H_{M_1} in detail, and solve the others by analogy.

We compute the Poisson bracket using H_{M_1}. The angular momentum vector evolves according to

$$\frac{d}{dt}\mathbf{M}=\mathbf{M}\times\nabla_{\mathbf{M}}H_{M_1}=\mathbf{M}\times\begin{pmatrix}\alpha_1 M_1\\0\\0\end{pmatrix} \tag{7.2.2}$$

or

$$\frac{d}{dt}\begin{pmatrix}M_1\\M_2\\M_3\end{pmatrix}=\begin{pmatrix}0\\\alpha_1 M_1 M_3\\-\alpha_1 M_1 M_2\end{pmatrix}. \tag{7.2.3}$$

These equations govern a rotation about the X axis with frequency $\alpha_1 M_1(0)$:

$$\mathbf{M}(t)=\begin{pmatrix}1&0&0\\0&\cos[\alpha_1 M_1(0)t]&\sin[\alpha_1 M_1(0)t]\\0&-\sin[\alpha_1 M_1(0)t]&\cos[\alpha_1 M_1(0)t]\end{pmatrix}$$

$$\mathbf{M}(0)=\mathsf{C}_X[\alpha_1 M_1(0)t]\mathbf{M}(0). \tag{7.2.4}$$

We obtain a similar equation for $\mathbf{R}$

$$\frac{d}{dt}\mathbf{R}=\mathbf{R}\times\begin{pmatrix}\alpha_1 M_1\\0\\0\end{pmatrix}, \tag{7.2.5}$$

and

$$\mathbf{R}(t)=\mathsf{C}_X[\alpha_1 M_1(0)t]\mathbf{R}(0). \tag{7.2.6}$$

The configuration matrix evolves according to:

$$\mathsf{C}(t)=\mathsf{C}(0)\mathsf{C}_X^{-1}[\alpha_1 M_1(0)t]. \tag{7.2.7}$$

Similarly, the Hamiltonians H_{M_2} and H_{M_3} lead to rotations about axis Y and Z:

(1) $H_{M_2}\rightarrow\mathbf{M}(t)=\mathsf{C}_Y[\alpha_2 M_2(0)t]\mathbf{M}(0)$;

$\mathsf{C}(t)=\mathsf{C}(0)\mathsf{C}_Y^{-1}[\alpha_2 M_2(0)t]$;

(2) $H_{M_3}\rightarrow\mathbf{M}(t)=\mathsf{C}_Z[\alpha_3 M_3(0)t]\mathbf{M}(0)$;

$\mathsf{C}(t)=\mathsf{C}(0)\mathsf{C}_Z^{-1}[\alpha_3 M_3(0)t]$,

where C_Y and C_Z refer to rotations about axis Y and Z, respectively.

7.3 The Free Rigid Body as We See It

The function $H_{\text{axisymmetric}}$ is the Hamiltonian of a body that is symmetric about Z; it was integrated in Sec. *7.1*. The function H_{triaxial} is a quadratic monomial of the form $H_{\text{triaxial}}=\alpha_1(M_1^2/2)$, where $\alpha_1=(1/I_1-1/I_2)$; it was integrated in Sec. *7.2*. Using the method of WH91, we construct algorithms for the integration of the motion of a free rigid body, by stringing together the parts we have just integrated. The order of the algorithms is limited only by the computational effort that one is willing to spend.

The scheme conserves the magnitude of $\mathbf{M}$: the motion is a composition of orthogonal transformations. Also, the scheme preserves the spatial angular momentum vector $\mathbf{m}$: in every step $\mathscr{B}$ and $\mathbf{M}$ rotate by equal and opposite amounts. It is also true that the mapping is symplectic and area preserving on the angular momentum sphere, since it was derived from the Lie–Poisson structure, which was derived by reducing the canonical Poisson bracket from the six-dimensional phase space to the sphere. The use of Cartesian coordinates avoids the singularities of Euler-type angles. Finally, the configuration of the rigid body is recovered naturally as part of the integration.

7.4 Stability Analysis of the Free Rigid Body Algorithm

We are interested in the stability of the rigid body algorithm. By that we mean the conditions under which the algorithm faithfully renders the actual motion. Since the algorithm is symplectic, and the angular momentum vector is restricted to a sphere, we know that, for small enough step size, the angular momentum vector will not drift on the sphere. It will either follow a closed curve, or be confined by such curves. However, the motion could still suffer from resonant interactions between the frequencies of the system and the step size of the mapping. Such resonances are best understood via the time-dependent Hamiltonian which our scheme integrates. In this section, we follow the work of Wisdom & Holman (1992) on the stability of symplectic mappings for the gravitational n-body problem. We study the Hamiltonian that generates the first-order mapping. We concentrate here on the primary resonances. The mapping Hamiltonian is

$$H_{\text{map}}=\frac{1}{2I_2}G^2+\frac{1}{2}\left(\frac{1}{I_3}-\frac{1}{I_2}\right)L^2-2\pi\delta_{2\pi}(\Omega t)\frac{1}{2}\left(\frac{1}{I_2}-\frac{1}{I_1}\right)\times(G^2-L^2)\sin^2(l). \tag{7.4.1}$$

As in previous sections, $\delta_{2\pi}(t)$ is a periodic sequence of Dirac delta functions, with period 2π and Ω is the mapping frequency. The step size of the integrator is given by $h=2\pi/\Omega$. The periodic delta functions admit a Fourier representation

$$\delta_{2\pi}(t)=\frac{1}{2\pi}\sum_{n=-\infty}^{\infty}\cos(nt), \tag{7.4.2}$$

which we incorporate into H_{map}:

$$H_{\text{map}}=\frac{1}{2I_2}G^2+\frac{1}{2}\left(\frac{1}{I_3}-\frac{1}{I_2}\right)L^2-\frac{1}{4}\left(\frac{1}{I_2}-\frac{1}{I_1}\right)(G^2-L^2)\times\sum_{n=-\infty}^{\infty}\cos(n\Omega t)+\frac{1}{4}\left(\frac{1}{I_2}-\frac{1}{I_1}\right)(G^2-L^2)\times\sum_{n=-\infty}^{\infty}\cos(2l-n\Omega t). \tag{7.4.3}$$

Because the total angular momentum G is conserved we can restrict our attention to the dynamics of the canonical pair (l,L), and ignore constant terms in the Hamiltonian. We can further simplify the Hamiltonian by factoring $1/I_3-1/I_2$ out, and rescaling time to get

© American Astronomical Society • Provided by the NASA Astrophysics Data System

1994AJ....107.1189T

$$H_{\rm map}=\frac{L^2}{2}-2\pi\delta_{2\pi}\left(\frac{\Omega}{\alpha}t\right)\frac{\gamma(G^2-L^2)}{4}+\frac{\gamma(G^2-L^2)}{4}\sum_{n=-\infty}^{n=\infty}\cos\left(2l-n\frac{\Omega}{\alpha}t\right), \quad (7.4.4)$$

where $\alpha=1/I_3-1/I_2$, and $\gamma=(1/I_2-1/I_1)/\alpha$. We will concentrate on the case where $\gamma\ll 1$, i.e., when the problem differs from an integrable one by a small time-dependent perturbation.

A primary resonance occurs whenever the argument of one of the cosines, in the Fourier expansion of $H_{\rm map}$, is stationary: $2(d/dt)l-n(\Omega/\alpha)=0$, for some $n\in\mathbf{Z}$. In order to study the motion near the nth primary resonance, we extract the resonance Hamiltonian:

$$H_{\rm res}=\frac{2+\gamma}{4}L^2+\frac{\gamma(G^2-L^2)}{4}\cos\left(2l-n\frac{\Omega}{\alpha}t\right), \quad (7.4.5)$$

and ignore the other terms. The resonance Hamiltonian contains one linear combination of angles. We can eliminate the time dependence with a canonical transformation, whose generating function is

$$F(L,\phi,t)=-\frac{1}{2}(L-L_r)\left(\phi+n\frac{\Omega}{\alpha}t\right), \quad (7.4.6)$$

where (p,ϕ) is the new canonical pair, and L_r is a constant to be determined. Explicitly, the transformation is given by

$$p=\frac{L-L_r}{2},$$

$$l=\frac{1}{2}\left(\phi+n\frac{\Omega}{\alpha}t\right). \quad (7.4.7)$$

Replacing in $H_{\rm res}$, we get a time-independent Hamiltonian:

$$\hat{H}_{\rm res}=H_{\rm res}+\frac{\partial F}{\partial t}=\frac{2+\gamma}{4}(2p+L_r)^2+\frac{\gamma[G^2-(2p+L_r)^2]}{4}\times\cos(\phi)-n\frac{\Omega}{\alpha}p. \quad (7.4.8)$$

Expecting small excursions away from the center of the resonance, we ignore terms of order γp and γp^2. We choose L_r to eliminate linear terms in p

$$L_r=\frac{n\Omega}{2\alpha}. \quad (7.4.9)$$

The momentum L_r gives the angular momentum at the resonance. Since $|L|\leqslant G$, we must have $(2|\alpha|G)/\Omega\geqslant 1$ for primary resonances to exist, or $h\geqslant h_0=\pi/|\alpha|G$. Ignoring the constant terms in $\hat{H}_{\rm res}$, we get

$$\hat{H}_{\rm res}=2p^2+\frac{\gamma(G^2-L_r^2)}{4}\cos(\phi) \quad (7.4.10)$$

The halfwidth of the libration region of this pendulum-like Hamiltonian is

$$p_{\rm max}=\frac{\sqrt{\gamma(G^2-L_r^2)}}{2}, \quad (7.4.11)$$

which we express in terms of the original variables

$$L_{\rm max}=2p_{\rm max}+L_r. \quad (7.4.12)$$

Notice that the maximum width is of the order of $\sqrt{\gamma}$.

Next, we look for the condition on Ω under which the separation between the resonance centers is equal to the sum of the halfwidth of their respective separatrices. This condition, known as the resonance overlap criterion, was used by Chirikov (1979) as a heuristic criterion for the development of chaos in nonintegrable problems. Since we are concerned with the numerical reliability of the method, we will worry about the overlap between the $n=0$ resonance, which enters the actual motion, and the $n=1$ resonance, which was introduced by the discretization. The condition for resonance overlap reads as follows:

$$2p_{\rm max}^{(0)}+2p_{\rm max}^{(1)}\geqslant|L_r^{(1)}|, \quad (7.4.13)$$

or,

$$\sqrt{\gamma}\left[G+\sqrt{G^2-\left(\frac{\Omega}{2\alpha}\right)^2}\right]\geqslant-\frac{\Omega}{2\alpha}. \quad (7.4.14)$$

In terms of the step size, the resonances will overlap when

$$h\geqslant h_{RO}=-\frac{\pi(1+\gamma)}{2\sqrt{\gamma}\alpha G}. \quad (7.4.15)$$

The evolution can be affected by step size resonances even if there is no serious resonance overlap. Thus, a more conservative limit on the step size of the map is to require that there are no primary step size resonances in the phase space: $h\leqslant h_0$.

7.5 Numerical Tests of the Free Rigid Body Algorithm

The numerical experiments discussed in this section are intended to illustrate the conservation properties of the rigid body algorithm, and the spurious resonances introduced by the discretization.

The continuous free rigid body motion conserves the kinetic energy. For an axisymmetric body, the mapping is exact, and consequently conserves the energy explicitly. However, for a triaxial body our free rigid body algorithm was not designed to explicitly conserve the energy. We expect that in this case the energy will oscillate with an amplitude that changes algebraically with the step size, for small enough step size. To illustrate this, we explored the dependence of the energy error on step size, with a first-order implementation of the algorithm. The behavior of the energy error as a function of time is shown in Fig. 1 for a rigid body which is close to axisymmetric: $I_1=0.5$, $I_2=0.51$, $I_3=1.0$. The initial conditions for this trajectory are: $M_2=0.0$, and $M_3=0.999$, with $M=1.0$. The step size is $h=0.01T_{\rm prec}$, where $T_{\rm prec}=2\pi/(\alpha M_3(0))$, and $\alpha=1/I_2-1/I_3$. As expected, the error oscillates and over the displayed time interval does not appear to grow secularly. As can be seen in the mapping Hamiltonian of the previous section, the smaller the triaxiality of the rigid body, the smaller the energy error at a given step size.

Of course, the amplitude of the energy error varies with the step size. For this first-order version of the algorithm,

© American Astronomical Society • Provided by the NASA Astrophysics Data System

1994AJ....107.1189T

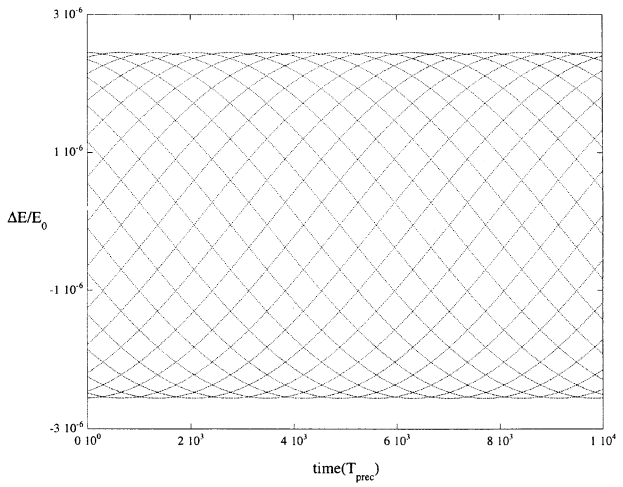

FIG. 1. The energy error in the free rigid body algorithm is plotted against time. The step size was set at 1/100 of the axisymmetric precession frequency, T_{prec}.

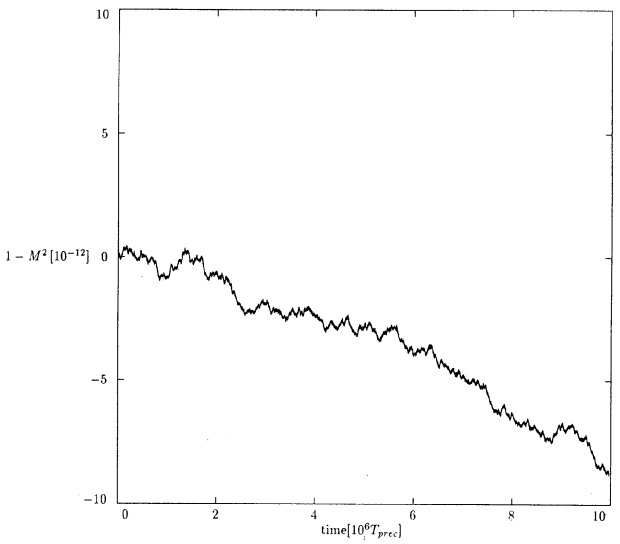

FIG. 3. A free rigid body was followed with a second-order algorithm. The error in the magnitude of the angular momentum vector is plotted against time.

the energy error is linear with step size for small step size. At large step sizes, step size resonances are encountered which give large energy errors. This behavior is illustrated in Fig. 2 for the same physical parameters and initial conditions as in the previous example. The maximum energy error over 5×10^3 iterations is plotted vs step size. The peaks in the energy error occur at step size resonances. Our stability analysis predicts primary resonances at step sizes $h/T_{\text{prec}}=nM_3(0)/2$. Figure 2 confirms the prediction.

Next we look at the conservation of the spatial angular momentum vector. Using the same rigid body but a second-order version of the algorithm, we consider a trajectory with $M_1(0)=0$, $M_2(0)=0.6$, $M_3(0)=0.8$, and an initial configuration which coincides with the inertial frame. The free body algorithm is designed to conserve the spatial angular momentum vector, **m**, and *a fortiori*, the magnitude of that vector. However, in practice, roundoff errors creep up on the integrals. As shown in Fig. 3, the magnitude of **m** differed from unity by $O(10^{-11})$ after a period of 10^7 T_{prec}. As far as the spatial components of **m**

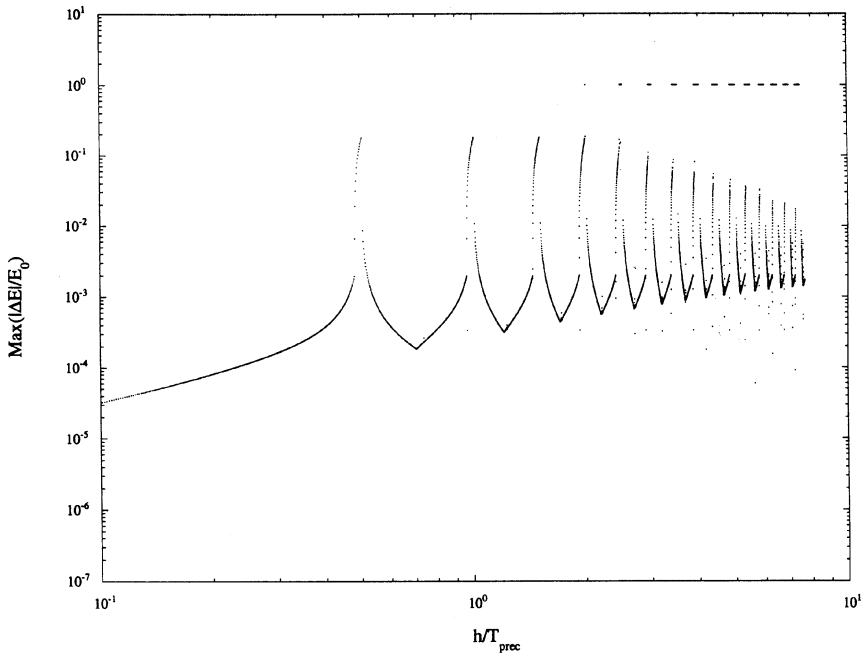

FIG. 2. The maximum energy error realized in 5×10^3 iterations, in a first-order algorithm, is plotted against the step size. Energy jumps occur at step sizes close to $nT_{\text{prec}}/2$, where n is the order of the primary resonance.

© American Astronomical Society • Provided by the NASA Astrophysics Data System

1994AJ....107.1189T

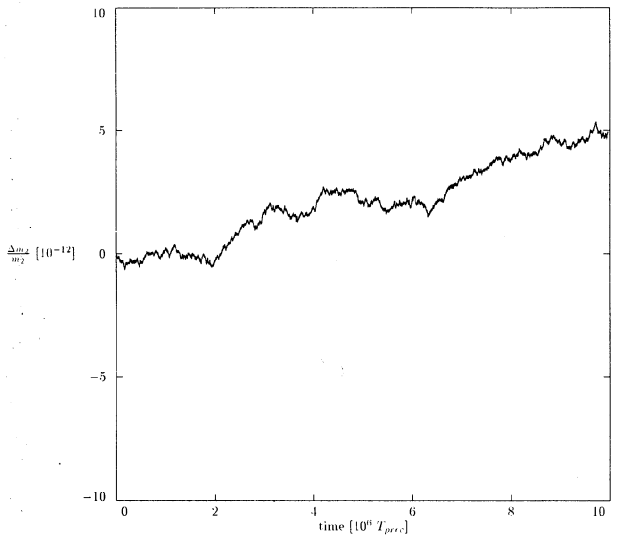

FIG. 4. The angular momentum of a free rigid body is fixed in space. Here, we plot the error in m_2, the y spatial component of the angular momentum vector, against time. In this experiment, the configuration is represented in terms of quaternions which are normalized every 100 steps.

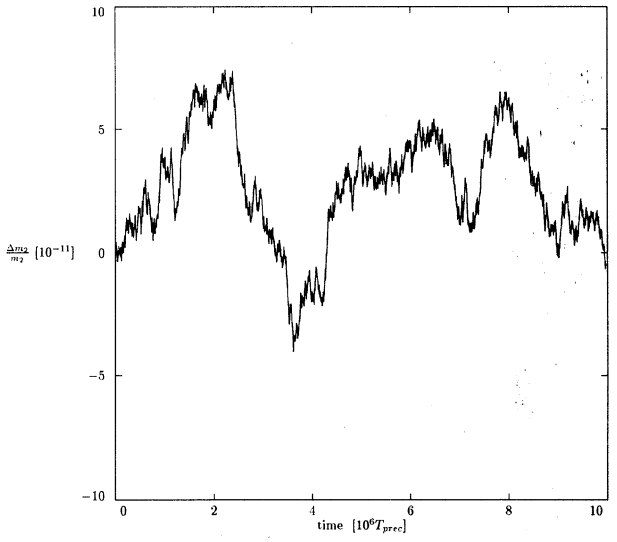

FIG. 5. The same experiment as in Fig. 4 was carried out except that in this case the configuration is represented in terms of standard rotations.

are concerned, they are affected both by roundoff errors in **M** and in the configuration. The configuration could be followed either in terms of the standard rotation matrices or in terms of the quaternions equivalent to them [see, e.g., Goldstein (1980)]. It is questionable whether quaternions alone can help cut down on the roundoff errors, since one pays the price for carrying four scalars (instead of the nine required for matrices) in terms of more involved algebraic operations. However, since our quaternions are of unit magnitude, we can enforce the special orthogonality of our transformations by normalizing at regular intervals. Typically, we find that by normalizing the quaternions, Fig. 4, we can cut roundoff errors by one order of magnitude below the maximum errors accrued when we used standard rotation matrices, Fig. 5. Thus, using normalized quaternions does cut down on roundoff error, but we suspect more improvement can still be made.

In summary, the energy integral is conserved to the order of the algorithm, as long as the chosen step size, for a given trajectory, avoids the artificial resonances. The angular momentum integrals suffer only from roundoff errors, and care must be taken to reduce them. Writing the evolution of the configuration in terms of quaternions is useful in the struggle against roundoff errors.

8. LIE–POISSON INTEGRATOR FOR A RIGID BODY IN THE FIELD OF A MASS POINT

Having developed algorithms for the free rigid body, we now turn to the solution of the interaction Hamiltonian $\hat{H}_{\text{interaction}}$

$$\hat{H}_{\text{interaction}}=-\frac{Gm_1}{2R^3}\,\text{tr}(\mathsf{I})+\frac{3}{2}\frac{Gm_1}{R^5}\,\mathbf{R}\cdot\mathsf{I}\mathbf{R} \tag{8.0.1}$$

to complete the full spin-orbit map.

Using the spin-orbit Lie–Poisson bracket, the equations of motion are

$$\frac{d}{dt}\mathbf{R}=0,$$

$$\frac{d}{dt}\mathbf{P}=-\frac{3Gm_1}{2R^5}\,\text{tr}(\mathsf{I})\mathbf{R}-\frac{3Gm_1}{R^5}\,\mathsf{I}\mathbf{R}+\frac{15Gm_1}{2R^7}\,(\mathbf{R}\cdot\mathsf{I}\mathbf{R})\mathbf{R}, \tag{8.0.2}$$

$$\frac{d}{dt}\mathbf{M}=\frac{3Gm_1}{R^5}\,\mathbf{R}\times\mathsf{I}\mathbf{R},$$

where tr(I) stands for the trace of the inertia tensor.

Since, $(d/dt)\mathbf{R}=0$, we trivially integrate the differential equations

$$\mathbf{R}(t)=\mathbf{R}(0),$$

$$\mathbf{P}(t)=\mathbf{P}(0)+[\nabla_{\mathbf{R}}\hat{H}_{\text{interaction}}]t, \tag{8.0.3}$$

$$\mathbf{M}(t)=\mathbf{M}(0)+[\mathbf{R}(0)\times\nabla_{\mathbf{R}}\hat{H}_{\text{interaction}}]t.$$

The forces and the torques are evaluated at $\mathbf{R}(0)$, the relative position vector in the body frame $\mathscr{B}$. Since the configuration is not affected by the evolution generated by $H_{\text{interaction}}$, we can assume that the configuration matrix at time t is given, and invert to get $\mathbf{R}(t)=\mathsf{C}^T(t)\mathbf{r}(t)$. It is natural to compute the Keplerian evolution in an inertial frame, so the change in the linear momentum in the inertial frame must be monitored

$$\mathbf{p}(t)=\mathbf{p}(0)+\mathsf{C}(t)[\mathbf{P}(t)-\mathbf{P}(0)]. \tag{8.0.4}$$

Having integrated all the components of the spin-orbit Hamiltonian, we are in a position to construct algorithms for the motion of a rigid body gravitationally interacting with a mass point. The simplest algorithm is first order in time and consists of a step of Kepler and Euler and a step of potential interactions. One can construct an algorithm

© American Astronomical Society • Provided by the NASA Astrophysics Data System

1994AJ....107.1189T

which is second order in time by taking a half-step of Eulerian and Keplerian motion, followed by a full step of potential interactions, and ending with a half-step of Eulerian and Keplerian motion. An Euler step updates the configuration of the rigid body which can then be used to compute the interactions in the rigid body frame.

If one is interested in a situation where the effect of the rigid body on the orbit of the mass point is negligible, then all that one has to do is to neglect the part of the interaction that affects the linear momenta. Of course, in that case, the total angular momentum is no longer conserved, but the orbital angular momentum is. Such a situation arises in the study of spin-orbit coupling in the solar system. It has been investigated in detail in Wisdom *et al.* (1984) and Wisdom (1987). Our algorithm presents an efficient tool for dealing with this problem.

As an algorithm for Lie–Poisson dynamics, ours echoes the generalizations of the ideas of Forest & Ruth (1990) given in Channell & Scovel (1991, hereafter referred to as CS91). These ideas are equivalent to the operator splitting approach given in WH91 with a different motivation. However, CS91 limit themselves, with Forest & Ruth (1990), to Hamiltonians which can be written as the sum of a kinetic and a potential energy. The approach of WH91 and our generalization to Lie–Poisson dynamics are not limited to such Hamiltonians. Also, CS91 do not consider the splitting of integrable problems into efficiently integrable subproblems, a step we exploit in our derivation. Further, the approach of WH91 has the added advantage of giving us a handle on the time-dependent Hamiltonian that is exactly integrated by the algorithm. This Hamiltonian can in turn be used to analyze the structure of the spurious resonances introduced by the algorithm as was done in Wisdom & Holman (1992) and carried out for the rigid body map in Sec. *7.4*. Finally, CS91 presented efficient implementations of the approach of Ge & Marsden (1988) which involves an approximation of the dynamics via generating functions. However, as pointed out by CS91 the explicit algorithms which use the operator splitting route are, in general, faster than algorithms that use the generating functions approach.

As an algorithm for rigid body dynamics, ours differs from the one presented in Austin *et al.* (1991) on the ground that our algorithm is Lie–Poisson while theirs, which is based on the midpoint rule, only preserves the Lie–Poisson structure to second order in the step size. The midpoint rule provides second-order algorithms which conserve integrals of motion which are linear or quadratic in the coordinates. In that sense, the algorithm of Austin *et al.* (1991) preserves both the energy and the angular momentum of the free rigid body. However, while it traces the trajectories on the sphere, it suffers from a systematic lag in the configuration space. Since our applications have an energy which is not quadratic in the coordinates, the midpoint rule will not preserve the energy anyway, and then it becomes advantageous to have the Lie–Poisson structure preserved. Further, Austin *et al.* (1991) do not provide higher-order generalizations of their algorithms. To our knowledge none of these rigid body algorithms have been generalized to spin-orbit problems as considered in this paper.

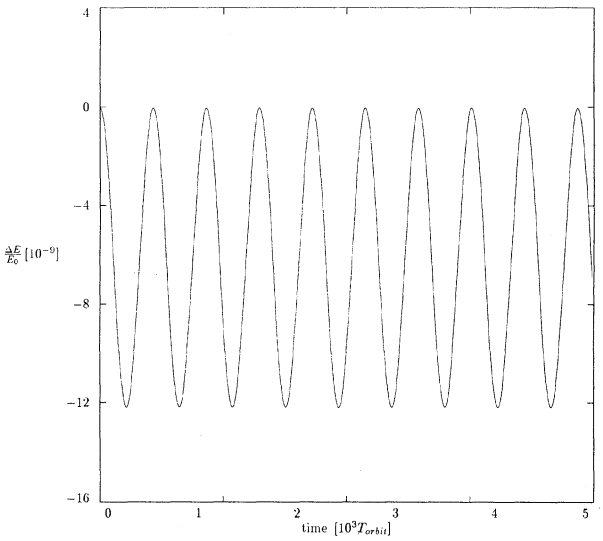

FIG. 6. The error in the Jacobi integral of a Moon-like body moving on a fixed circular orbit is plotted against time.

8.1 Energy Conservation in the Spin-Orbit Integrator

We explore the energy conservation properties of the spin-orbit coupling algorithm. In most solar system applications, the rotational energy is negligible when compared to the orbital energy. To get a handle on the rigid body contribution to the energy, we look at a rigid body moving on a fixed Keplerian orbit. Of course, in this case, neither the total energy nor the total angular momentum vector are conserved. However, by choosing the orbit to be circular, and moving to a frame that is rotating at the orbital rate, we get rid of the periodic time dependence, and obtain a "Jacobi"-like integral which captures the contribution of rigid body interactions to the energy [see Wisdom (1987)]. As an example we considered a body with the Moon's moments of inertia which is moving on a fixed circular orbit and used a second-order version of the algorithm. We started the body spinning at the orbital frequency about the axis with largest principal moment, and tipped that axis 0.1 radians with respect to the orbit normal. We monitored the variation in the integral of the motion over a time span of 5000 orbits, with a step size of 1/100 of the orbital period. The result is shown in Fig. 6. The error in energy oscillates and shows no signs of secular growth, a commonly observed feature of symplectic integrators. We carried out a similar experiment with an axisymmetric Mars-like body spinning about the axis with largest principal moment at Mars' current rotational period and attitude. With a step size of 1/100 of the orbital period, the energy oscillates with an amplitude of order 10^{-11} as can be seen in Fig. 7.

© American Astronomical Society • Provided by the NASA Astrophysics Data System

1994AJ....107.1189T

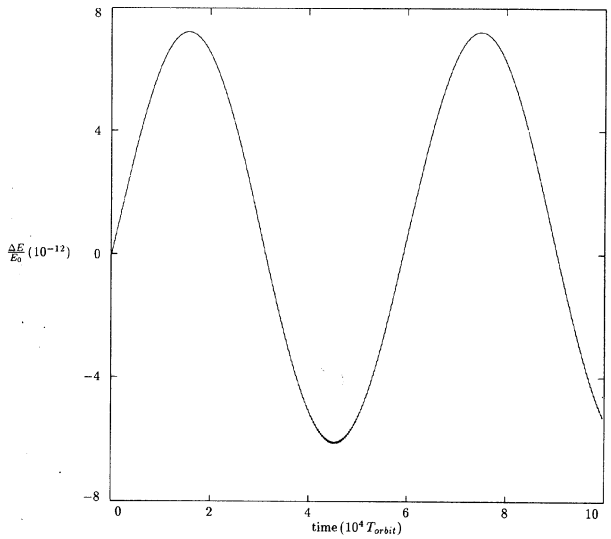

FIG. 7. The error in the Jacobi integral of a Mars-like body moving on a fixed circular orbit is plotted against time.

9. GENERALIZATIONS: THE DYNAMICS OF RIGID BODIES IN THE SOLAR SYSTEM

Now that we have derived a mapping for following the motion of a rigid body gravitationally interacting with a mass point, it is a simple matter to generalize to more complicated situations.

9.1 One Rigid Body in the Gravitational n-Body Problem

The step from one mass point and a rigid body to n mass points and a rigid body increases the computational effort, but leaves the conceptual framework practically unchanged. The Hamiltonian of this problem is given by

$$H=\frac{1}{2}\mathbf{M}\cdot\mathsf{I}^{-1}\mathbf{M}+\sum_{i=0}^{n}\frac{\mathbf{p}_i^2}{2m_i}-\sum_{0<i<j}^{n}\frac{Gm_im_j}{r_{ij}}-\sum_{\substack{i=0\\ i\neq 1}}^{n}\int_B\frac{Gm_i}{|r_{i1}+\mathsf{C}\mathbf{Q}|}\,dm(\mathbf{Q}), \tag{9.1.1}$$

where, in this case, the massive central body has index 0 and the rigid body has the index 1. We carry out the following operations on the Hamiltonian.

(1) Transform the Hamiltonian to heliocentric (or Jacobi) coordinates to eliminate the center of mass motion.

(2) Further transform the Hamiltonian by moving to a frame rotating with the rigid body.

(3) Expand the potential interaction between the rigid body and the mass points in terms of Legendre polynomials and keep, as before, three terms of the expansion.

(4) Group into two separate Hamiltonians the terms governing the free motion (Keplerian and Eulerian), and the interactions (translational and rotational).

We work in a heliocentric framework since it is natural for computing the rigid body interactions. We carry out the steps outlined above and end up with the following Hamiltonian:

$$\hat{H}=\hat{H}_{\text{Kepler}}+\hat{H}_{\text{Euler}}+\hat{H}_{\text{interactions}}+\hat{H}_{\text{indirect}}, \tag{9.1.2}$$

where

$$\begin{aligned}\hat{H}_{\text{Kepler}}&=\sum_{i=1}^{n}\left(\frac{\mathbf{P}_i^2}{2\mu_i}-\frac{Gm_0m_i}{R_{0i}}\right),\\ \hat{H}_{\text{Euler}}&=\frac{M_1^2}{2I_1}+\frac{M_2^2}{2I_2}+\frac{M_3^2}{2I_3},\\ \hat{H}_{\text{interactions}}&=-\sum_{0<i<j}^{n}\frac{Gm_im_j}{R_{ij}}\\ &\quad-\sum_{\substack{i=0\\ i\neq 1}}^{n}\left(\frac{Gm_i}{2R_{i1}^3}\,\mathrm{tr}(\mathsf{I})-\frac{3}{2}\frac{Gm_i}{R_{i1}^5}\mathbf{R}_{i1}\cdot\mathsf{I}\mathbf{R}_{i1}\right),\\ \hat{H}_{\text{indirect}}&=\frac{1}{2m_0}\sum_{\substack{i,j=1\\ j\neq i}}^{n}\mathbf{P}_i\cdot\mathbf{P}_j,\end{aligned} \tag{9.1.3}$$

where $1/\mu_i=1/m_i+1/m_0$.

We note that the Lie–Poisson bracket that we derived for the case of a rigid body interacting with one mass point generalizes naturally to the case of n mass points. The reduction was made possible by moving to the rigid body frame, a step we can still take in this problem. All we have to do is to account for the additional torques on the body and the reaction forces on the mass points

$$\begin{aligned}\frac{d}{dt}\mathbf{R}_{0i}&=\{\mathbf{R},\hat{H}\}=\mathbf{R}_{0i}\times\nabla_{\mathbf{M}}\hat{H}+\nabla_{\mathbf{P}_i}\hat{H},\\ \frac{d}{dt}\mathbf{P}_i&=\{\mathbf{P},\hat{H}\}=\mathbf{P}_i\times\nabla_{\mathbf{M}}\hat{H}-\nabla_{\mathbf{R}_{0i}}\hat{H},\quad i=1,\ldots,n,\\ \frac{d}{dt}\mathbf{M}&=\{\mathbf{M},\hat{H}\}=\mathbf{M}\times\nabla_{\mathbf{M}}\hat{H}+\sum_{j=1}^{n}\mathbf{R}_{0j}\times\nabla_{\mathbf{R}_{0j}}\hat{H}.\end{aligned} \tag{9.1.4}$$

The Keplerian motion is found by using a Kepler solver like the one discussed in WH91. The Eulerian free body motion is solved using the Lie–Poisson algorithm we presented above. The Hamiltonian H_{indirect} results from the transformation to the noninertial heliocentric frame. Since it only depends on the linear momenta, it will only affect the position vectors

$$\mathbf{R}_{0i}(t)=\mathbf{R}_{0i}(0)+\frac{t}{m_0}\sum_{\substack{j=1\\ j\neq i}}^{n}\mathbf{P}_j,\quad i=1,\ldots,n. \tag{9.1.5}$$

The interaction Hamiltonian depends on the relative distances between the various objects. Thus, as before, this Hamiltonian affects the momenta only, leaving the position vectors and the configuration of the rigid body unchanged. We integrate it to get

© American Astronomical Society • Provided by the NASA Astrophysics Data System

1994AJ....107.1189T

$$\mathbf{R}_{0i}(t)=\mathbf{R}_{0i}(0),$$

$$\mathbf{P}_i(t)=\mathbf{P}_i(0)-[\nabla_{\mathbf{R}_{0i}}\hat{H}_{\text{interaction}}]t, \quad i=1,\ldots,n, \qquad (9.1.6)$$

$$\mathbf{M}(t)=\mathbf{M}(0)+\left(\sum_{\substack{j=0\\ j\neq 1}}^{n}\mathbf{R}_{j1}(0)\times\nabla_{\mathbf{R}_{j1}}\hat{H}_{\text{interaction}}\right)t,$$

where the forces and torques are evaluated at $\mathbf{R}_{0i}(0)$, $i=1,\ldots,n$.

This completes the integration of the parts. Finally, we construct a mapping that approximates solutions to the full Hamiltonian by following the method of WH91. A second-order mapping will consist of: a half-step along $H_{\text{interactions}}$ which modifies the momenta; a half-step along H_{indirect}, which modifies the position vectors; a full step of Keplerian and Eulerian motion; a half-step H_{indirect} with the current momenta, and a final half-step of $H_{\text{interactions}}$.

9.2 Two or More Rigid Bodies in the Gravitational n-Body Problem

This case generalizes the previous one. We will be interested in cases where the first three Legendre polynomials in the potential expansion are sufficient. This allows us to ignore rigid–rigid interactions, or equivalently, to assume that each rigid body sees all the other bodies in the system as mass points. Thus, the problem reduces to the previous one, except that we have to follow two or more angular momentum vectors and configurations instead of one.

10. SUMMARY

We derived a symplectic integrator for a free rigid body, which conserves the magnitude of the angular momentum vector and its orientation in space. Two equivalent versions were discussed: one made use of a canonical Poisson structure, the other of the Lie–Poisson structure of a free rigid body. Numerical experiments explored the conservation properties of the algorithm. Roundoff errors were reduced by using a quaternion formulation, with timely normalization. The energy error was bounded, and suffered from large increases at resonant step sizes. The time-dependent Hamiltonian, which generates the algorithm, was used to analyze the primary resonances introduced by the discretization. The free rigid body integrator was incorporated in the n-body integrator of WH91, to provide a mapping for the dynamics of one or more rigid bodies interacting gravitationally with mass points. This mapping is Lie–Poisson in the sense that it preserves the Poisson structure and the symmetries generated by the Lie group of Euclidean transformations.

We thank M. Holman for his invaluable support during all the stages of the project, and A. Toomre and S. Tremaine for helpful discussions. We thank J. Marsden, J. C. Simo, and S. Wiggins for discussions on symplectic integrators.

REFERENCES

Abelson, H., Berlin, A. A., Katzenelson, J., McAllister, W. H., Rozas, G. J., Sussman, G. J., & Wisdom, J. 1992, preprint
Andoyer, H. 1923, Cours de Mechanique Celeste, Vol. 1 (Gauthier-Villars, Paris)
Arnold, V. I. 1966, Ann. Inst. Fourier, Grenoble, 16, 319
Arnold, V. I. 1978, Mathematical Methods of Classical Mechanics (Springer, New York)
Austin, M. A., Krishnaprasad, P. S., & Wang, L.-S. 1991, SRC Technical Report, Systems Research Center, University of Maryland, College Park, MD 20742
Channell, P. J., & Scovel, J. C. 1991, Physica D, 50, 80
Chirikov, B. V. 1979, Phys. Rep., 52, 263
Danby, J. M. A. 1988, Fundamentals of Celestial Mechanics (Willmann–Bell, Richmond)
Deprit, A. 1967, Am. J. Phys., 35, 424
Forest, E., & Ruth, R. D. 1990, Physica D, 43, 105
Ge, Z., & Marsden, J. E. 1988, Phys. Lett. A, 133, 134
Goldstein, H. 1980, Classical Mechanics, 2nd ed. (Addison–Wesley, Reading)
Laskar, J. 1989, Nature, 338, 237
Plummer, H. C. 1960, An Introductory Treatise on Dynamical Astronomy, (Dover, New York)
Sussman, G. J., & Wisdom, J. 1992. Sci, 257, 56
Wang, L.-S., Krishnaprasad, P. S., & Maddocks, J. H. 1991, Celestial Mechanics and Dynamical Astronomy, 50, 349
Wisdom, J., Peale, S. J., & Mignard, F. 1984, Icarus, 58, 137
Wisdom, J. 1987, AJ, 94, 1350
Wisdom, J., & Holman, M. 1991, AJ, 102, 1528
Wisdom, J., & Holman, M. 1992, AJ (submitted)

© American Astronomical Society • Provided by the NASA Astrophysics Data System